DOI 10.1007/s12182-012-0199-4

Modeling CO_2 miscible flooding for enhanced oil recovery

Ju Binshan[1, 2*], Wu Yu-Shu[3], Qin Jishun[4], Fan Tailiang[1, 2] and Li Zhiping[1, 2]

[1] School of Energy Resources, China University of Geosciences (Beijing), Beijing, 100083, China

[2] Key Laboratory of Marine Reservoir Evolution and Hydrocarbon Accumulation Mechanism, Ministry of Education, China University of Geosciences (Beijing), Beijing 100083, China

[3] Colorado School of Mines, USA

[4] PetroChina Research Institute of Petroleum Exploration and Development, Beijing 100083, China

Abstract: The injection of fuel-generated CO_2 into oil reservoirs will lead to two benefits in both enhanced oil recovery (EOR) and the reduction in atmospheric emission of CO_2. To get an insight into CO_2 miscible flooding performance in oil reservoirs, a multi-compositional non-isothermal CO_2 miscible flooding mathematical model is developed. The convection and diffusion of CO_2-hydrocarbon mixtures in multiphase fluids in reservoirs, mass transfer between CO_2 and crude, and formation damages caused by asphaltene precipitation are fully considered in the model. The governing equations are discretized in space using the integral finite difference method. The Newton-Raphson iterative technique was used to solve the nonlinear equation systems of mass and energy conservation. A numerical simulator, in which regular grids and irregular grids are optional, was developed for predicting CO_2 miscible flooding processes. Two examples of one-dimensional (1D) regular and three-dimensional (3D) rectangle and polygonal grids are designed to demonstrate the functions of the simulator. Experimental data validate the developed simulator by comparison with 1D simulation results. The applications of the simulator indicate that it is feasible for predicting CO_2 flooding in oil reservoirs for EOR.

Key words: Compositional simulator, CO_2 flooding, mathematical model, irregular grids

1 Introduction

Since 1750, the CO_2 concentration in the atmosphere has increased from 280 ppm to 368 ppm in 2000, and 388 ppm in 2010 (Rackley, 2010). Chinese annual CO_2 emission was 5.1 billion tonnes at 2005, and it will reach 8.6 billion tonnes at 2020 (Wang et al, 2011).

The CO_2 emission is increasing at an average rate of 4.5% per annum. The increase in atmospheric emission of CO_2 with the attendant global warming and environmental degradation are driven by global energy demand.

Depleted or mature oil and gas fields may provide favorable sites for storing CO_2 in porous and permeable reservoirs (Wells et al, 2007; Özkilic and Gumrah, 2009; Yang et al, 2010). In most oil reservoirs, CO_2 exists as a supercritical fluid under reservoir conditions, which is a favorable flooding agent for enhanced oil recovery (EOR). Studies (Adewusi, 1998; Farajzadeh et al, 2009) show that CO_2 flooding for EOR in oil fields can improve oil recovery significantly. Miscible CO_2 flooding is capable of mixing in any ratio without separation of CO_2 and oil phases, and immiscible CO_2 flooding leads to CO_2 and oil phases because of CO_2 cannot be completely be dissolved in oil. Miscible flood is better than immiscible flood for CO_2 as it has more displacement efficiency for crude oil in a miscible (supercritical) state. CO_2 has been injected into the oil formations of many oil fields in the world for EOR (Orr et al, 1982; Mungan, 1992; Barnhart and Coulthard, 2000; Dahaghi et al, 2008).

During the CO_2 miscible flooding process in oil reservoirs, the main mechanism includes 1) miscible displacement, 2) convection and diffusion, 3) phase behavior of in-situ fluids on flow and mass transfer, 4) heavy organic precipitation and its effects on porosity and permeability, and 5) reducing oil viscosity.

Song (2008) studied the main factors that influence CO_2 miscible displacement using numerical simulation. However, the research is not based on his own simulator, and no mathematical model was presented in his work. More recently, Su et al (2011) developed a one-dimensional mathematical model for CO_2 miscible displacement with CO_2 adsorption. However, energy transfer was not considered in this model, and the oil is treated as one component. Therefore, the model is not a compositional model.

In this paper, the authors develop a non-isothermal

*Corresponding author. email: jubs2936@163.com
Received November 4, 2011

compositional mathematical model. The changes in porosity and permeability caused by asphaltene precipitation are considered in the model. The integral finite difference method that is used to discretize in space and time is discretized as a fully implicit finite-difference. A reservoir simulator is developed to predict CO_2 miscible flooding behavior. Two simulation samples are designed to demonstrate the functions of the simulator. It is found that the predicted recovery from CO_2 injection under miscible conditions has a good match with the slim tube experimental recovery.

2 Mathematical model and governing equations

2.1 Assumption and consideration in the model

CO_2 flow and transport in porous media are simulated using a conceptual model of multiphase fluid flow and multi-component transport within oil and water. The CO_2-EOR mathematical model is based the following assumptions:

1) Heterogeneity of the oil formation and compressibility are considered.

2) Heat transfer in porous media is considered.

3) Flow and transport mechanisms include multiphase Darcy flow and multi-component diffusion, subject to adsorption and precipitation.

4) Mass components include CO_2, H_2O, and oil with some pseudo-oil components.

5) The flooding process is miscible.

6) CO_2 adsorption on pore walls of the oil formation is considered.

7) Formation damage induced by asphaltene deposition on pore walls is considered.

2.2 Governing equations

The physical processes associated with CO_2, oil, and water flow and transport in porous media are governed by the same fundamental conservation laws. Conservation of mass, momentum, and energy govern the behavior of fluid flow and heat transfer in rock. These physical laws are often represented mathematically on the macroscopic level by a set of partial differential or integral equations. We assume that these processes can be described using a continuum approach within a representative elementary volume (REV) in a porous medium.

2.2.1 Mass conservation equations

According to the mass conservation law, a conservation equation of mass components in the porous media can be written as follows:

$$\frac{\partial A^k}{\partial t} = F^k + q^k \tag{1}$$

where superscript k is the index for the components, k = 1, 2, 3, … N_c, with N_c being the total number of mass components; A^k is the accumulation term of component k, kg/m^3; q^k is an external source/sink term for mass component k, kg/(s·m^3); and F^k is the "flow" term of mass, or diffusive and dispersive mass transport, kg/(s·m^3).

The accumulation terms in Eq. (1) for component k is written as

$$A^k = \phi \sum_{\beta} \left(\rho_\beta S_\beta X_\beta^k \right) + R_s^k \qquad (k = 1, 2, 3, \ldots, N_c) \tag{2}$$

where subscript β is an index for fluid phase (β = g for gas phase, = w for aqueous phase, = o for oil phase); ϕ is the porosity of porous media; ρ_β is the density of phase β, kg/m^3; and S_β is the saturation of phase β; X^K_β is the mole fraction of component k in fluid β; R_s^k is the adsorption term of component k on rock solids, kg/m^3.

The adsorption term in Eq. (2) is used mainly for incorporating possible CO_2 adsorption and may be described using a K_d approach,

$$R_s^k = \int_0^t \rho_\beta \frac{\partial \delta^k}{\partial t} = \int_0^t \rho_\beta \alpha_d^k v_o X_\beta^k \, \mathrm{d}t \qquad (k = 1, 2, 3, \ldots, N_c) \tag{3}$$

where α_d^k is a capture rate constant of component k at pore walls, kg/m; v_o is the flow velocity of the oil phase, m/s; δ^k is the volume of component k deposited on the pore surfaces per unit bulk volume. Some heavy components such as asphalt and asphaltene have more opportunity to attach on pore walls, which leads to formation damage.

The mass component transport is governed in general by processes of advection, diffusion and dispersion. The total mass flow term (Scheidegger, 1961; Wu and Pruess, 2000) for a component k, by advection and dispersion, is written as

$$F^k = -\sum_{\beta} \nabla \bullet \left(\rho_\beta X_\beta^k v_\beta \right) + \sum_{\beta} \nabla \bullet \left(\underline{D}_\beta^k \bullet \nabla \left(\rho_\beta X_\beta^k \right) \right) \qquad (k = 1, 2, 3, \ldots, N_c) \tag{4}$$

where v_β is a vector of volumetric flow rate for fluid flow, defined by Darcy's law to describe the multiphase flow as,

$$v_\beta = -\frac{\kappa \kappa_{r\beta}'}{\mu_\beta} \left(\nabla P_\beta - \rho_\beta g \nabla z \right) \tag{5}$$

where P_β (Pa), μ_β (Pa·s), and g (m/s^2) are pressure, viscosity of fluid phase β, and gravitational constant, respectively; z is the vertical coordinate; κ is the absolute or intrinsic permeability, m^2; and $\kappa_{r\beta}$ is the relative permeability to phase β. In Eq. (4), $\underline{D}_\beta^k$ is the hydrodynamic dispersion tensor accounting for both molecular diffusion and mechanical dispersion for component k in phase β, m^2/s, defined by an extended dispersion model (Scheidegger, 1961) to include multiphase effects (Wu and Pruess, 2000) as,

$$\underline{D}_\beta^k = \alpha_T^\beta \left| v_\beta \right| \delta_{ij} + \left(\alpha_L^\beta - \alpha_T^\beta \right) \frac{v_\beta v_\beta}{\left| v_\beta \right|} + \phi S_\beta \tau d_\beta^k \delta_{ij} \qquad (k = 1, 2, 3, \ldots, N_c) \tag{6}$$

where α_T^β and α_L^β are the transverse and longitudinal dispersivities, respectively, in fluid β of porous media, m; τ is the tortuosity of the porous medium; d_β^K is the molecular diffusion coefficient of component k within fluid β, m^2/s; and δ_{ij} is the Kronecker delta function (δ_{ij} = 1 for $i = j$, and δ_{ij} = 0 for $i \neq j$), with i and j being coordinate indices.

2.2.2 Energy conservation equations

Heat transfer in porous media is in general a result of both convective and conductive heat-transfer processes (Scott, et al 2005; Dabagh et al, 2009), and radiation may be ignored in most cases. These heat-transfer processes are complicated by interactions between multiphase fluids, multicomponents, and associated changes in phases, internal energy, and enthalpy. The combined, overall heat flux term, from convection, conduction and radiation in a multiphase, multicomponent, porous medium system, may be described as,

$$\frac{\partial}{\partial t}\left\{\sum_{\beta}\left(\phi\,\rho_{\beta}S_{\beta}U_{\beta}\right)+\left(1-\phi\right)\,\rho_{\mathrm{s}}U_{\mathrm{s}}\right\}-q^{T}= -\sum_{\beta}\nabla\bullet\left(h_{\beta}\,\rho_{\beta}\,v_{\beta}\right)+\sum_{\beta}\;\sum_{k}\nabla\bullet\left(\;h_{\beta}^{k}\underline{D}_{\beta}^{k}\bullet\nabla\left(\rho_{\beta}X_{\beta}^{k}\right)\right) +\nabla\bullet\left(C_{\mathrm{T}}\nabla T\right) \tag{7}$$

where ρ_s is the density of rock solids, kg/m^3; and U_β and U_s are the internal energies of fluid β and rock solids, respectively, J/kg; q^T are external source/sink terms for component k and energy, W/(s·m^3); h_β and h_β^k are specific enthalpies of fluid phase β and of component k in fluid β, respectively, J/kg; C_T is the overall thermal conductivity, W/(m·ºC); and T is the temperature, ºC.

2.2.3 Constitutive relationships

To complete the mathematical description of multiphase flow and heat transfer in porous media, the mass and energy-balance equation needs to be supplemented with a number of constitutive equations. The constitutive correlations are expressed as follows.

Constraint on summation of total fluid saturation in porous media satisfies as

$$\sum_{\beta}S_{\beta}=1 \tag{8}$$

Constraint on mole fractions within phase β is written as

$$\sum_{k}X_{\beta}^{k}=1 \tag{9}$$

2.2.4 Description of formation damage

The adsorption of heavy components on pore surfaces may lead to the changes in the local porosity and permeability of the oil formation (Ju et al, 2009). The instantaneous porosity is expressed by

$$\phi=\phi-\Delta\phi \tag{10}$$

where $\Delta\phi$ denotes the variation of porosity by retention of heavy components in porous media, and it is expressed by

$$\Delta\phi=\sum\delta^{k} \tag{11}$$

The change in permeability in this study is caused by asphaltene release and mobilization. According to the literature (Ju et al, 2007), the expression for instantaneous permeability changed by release and retention of asphaltene is given by

$$\kappa\;=\kappa_{0}[(1-f)\lambda_{f}+f\phi/\phi_{0}]^{n} \tag{12}$$

in which κ_0 and ϕ_0 are the initial permeability (m^2) and porosity; κ and ϕ are the instantaneous local permeability (m^2) and porosity of porous media; and λ_f is a constant for fluid seepage allowed by the plugged pores. The range of index n is from 2.5 to 3.5. f is a flow efficiency factor (Ju et al, 2002).

3 Numerical solution scheme

3.1 Selection of primary variables and variable switching

There are a total of N_c mass conservation equations to solve for an isothermal reservoir; and N_{c+1} equations to solve for a non-isothermal system. The selection of primary variables lists in Table 1.

Table 1 Primary parameters and variables in the Jacobian matrix

Index	1	2	3	4	…	m	...	N_c–1	N_c	N_c+1
Parameters	P_O	X_O^3	X_O^4	X_O^5	…	…	…	$X_O^{N_c}$	S_w	T
Variables in the Jacobian matrix	x_1	x_2	x_3	x_4	…	x_m	…	x_{N_c-1}	x_{N_c}	x_{N_c+1}

In Table 1, subscript o denotes the phase index for oil; and X_O^k is the mole fraction of component k in the oil phase.

3.2 Discretization and numerical solution procedure

Time discretization is carried out using a backward, first-order, fully implicit finite-difference scheme and the integral finite-difference method (Pruess et al, 1999) is used for spatial discretization. The discrete nonlinear equations for the mass and heat of component k at node i can be written in a general form:

$$\left\{A_i^{k,n+1}-A_i^{k,n}\right\}\frac{V_i}{\Delta t}=\sum_j flow_{ij}^{k,n+1}+Q_i^{k,n+1} \tag{13}$$

where k = 1, 2, 3, …, N_c, N_c+1 (N_c+1 denotes energy equation), and i =1, 2, 3,…, N.

There are a number of numerical solution techniques that have been developed in the literature over the past few decades to solve the nonlinear, discrete equations of reservoir simulations. The predominant approach is to use a fully implicit scheme. This is due to the extremely high nonlinearity inherent in those discrete equations which causes convergence difficulties. The discrete non-linear equation (Eq. (13)) can be written in a residual form:

$$R_i^{k,n+1}=\left\{A_i^{k,n+1}-A_i^{k,n}\right\}\frac{V_i}{\Delta t}-\sum_j flow_{ij}^{k,n+1}-Q_i^{k,n+1}=0 \tag{14}$$

In terms of the primary variables, the residual equation (Eq. (14)) at node i is regarded as a function of the primary variables at not only node i, but also at all its direct neighboring nodes j. The Newton iteration scheme gives rise to:

$$\sum_m \frac{\partial R_i^{k,n+1}\left(x_{m,p}\right)}{\partial x_m}\left(\delta x_{m,p+1}\right) = -R_i^{k,n+1}\left(x_{m,p}\right) \quad (15)$$

where x_m is the primary variable m with m = 1, 2, 3, …, N_{c+1}, respectively, at node i and all its direct neighbors; p is the iteration level; and i =1, 2, 3, …, N. The primary variables in Eq. (15) need to be updated after each iteration:

$$x_{m,p+1} = x_{m,p} + \delta x_{m,p+1} \quad (16)$$

The Newton iteration process continues until the residuals $R_i^{k,n+1}$ or changes in the primary variables $\delta x_{m,p+1}$ over an iteration are reduced below preset convergence tolerances.

4 Numerical results and discussion

This section will demonstrate the functions of the simulator and validate the mathematical model that predicts CO_2 miscible flooding.

4.1 The comparison between simulation and slim tube experimental data

The simulation result of one-dimensional miscible flooding was compared with the slim tube experimental data. The main parameters used in numerical simulation are shown in Table 2. The minimum miscible pressure (MMP) of the CO_2-oil system is 27.9 MPa, which was also obtained by slim tube experiments in the laboratory. The crude oil used in MMP and CO_2 flooding experiments was sampled from well H75-29-5 in the Honggang Oil Field. The viscosity and density at reservoir conditions were 1.67 mPa·s and 0.7464 g/cm^3. The initial model pressure and flow pressure at the outlet (the 30th grid) were set at 32.50 MPa and 31.90 MPa, which keep miscible flooding during the simulation. The conditions such as pressure and temperature were kept the same in the numerical run and experiments.

Table 2 Main parameters of the example

Parameters	Value
The length of the slim tube, m	18.30
The node numbers	30
The size of grid of x, m	0.61
Temperature, ºC	108.30
Initial pressure, MPa	32.50
Number of pseudo-components of crude oil	5
Cross-section area of the model, 10^{-5} m^2	1.169
Initial oil saturation	0.77
Connate water saturation	0.23
Initial gas saturation	0
Porosity	0.39
Permeability, μm^2	3.20
CO_2 injection rate, 10^{-8} kg/s	2.5
Wellhole flow pressure, MPa	31.90

Fig. 1 shows that the oil recovery increases approximately linearly with continuous injection of CO_2 until 0.90 pore volume (PV) of CO_2 has been injected. Then the increase in the oil recovery slows down because of CO_2 breakthrough at the outlet of the model. The oil recoveries obtained by the simulation match well with experimental data. There is only a small deviation between the numerical and experimental results, which validates the reliability of the mathematical model.

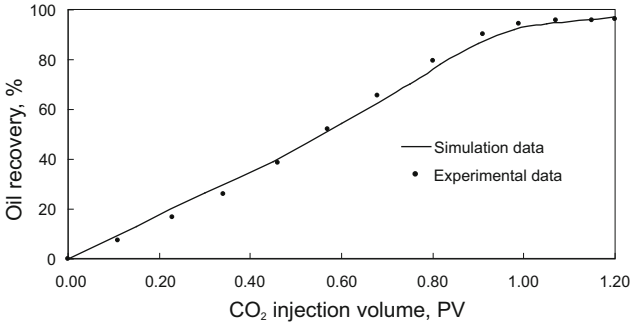

Fig. 1 A comparison between numerical results and experimental data

Fig. 2 shows the distribution of CO_2 in the oil phase along the model from the inlet to the outlet. This indicates that CO_2 arrives at the outlet before 0.90 PV of CO_2 has been injected. Fig. 3 demonstrates the distributions of each component (five pseudo-components for hydrocarbon) along the model when 0.33 PV of CO_2 is injected. This implies that the hydrocarbon components are displaced from the locations where the CO_2 has swept. There is a relative flat displacement front for the diffusion phenomenon. The simulation results imply that CO_2 flooding is piston-like displacement in the miscible state, which leads to a high displacement efficiency. Zhao et al (2011) drew a similar conclusion from flooding experiments.

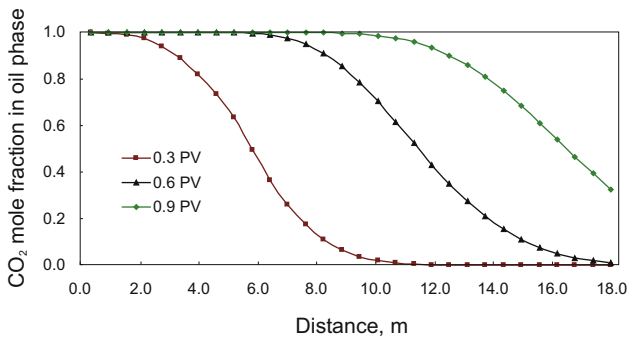

Fig. 2 CO_2 distribution in the oil phase at different injection volumes

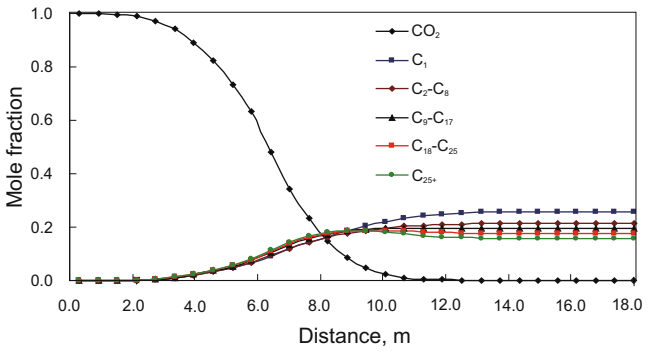

Fig. 3 Distributions of each component in the oil phase after 0.33 PV of CO_2 injected

4.2 Three dimensional sample

This section is designed to demonstrate the grid types and their effects on CO_2 distribution in the oil phase. Due to the application of the integral finite difference technique in the discretization for the governing equation, the regular grid (cuboids) or flexible irregular grid type (polygonal, PEBI, hybrid, etc.) is optional for a simulation. Fig. 4 shows the two types of grid used as demonstration examples for CO_2 miscible flood for EOR in a five-spot well pattern. Fig. 4 (a) is a regular cuboidal grid model and Fig. 4 (b) is a hybrid grid system with locally refined grids around injection and production wells. The geological and other parameters such as reservoir fluids are completely the same except for grid discretization for the two demonstrations (see Table 3).

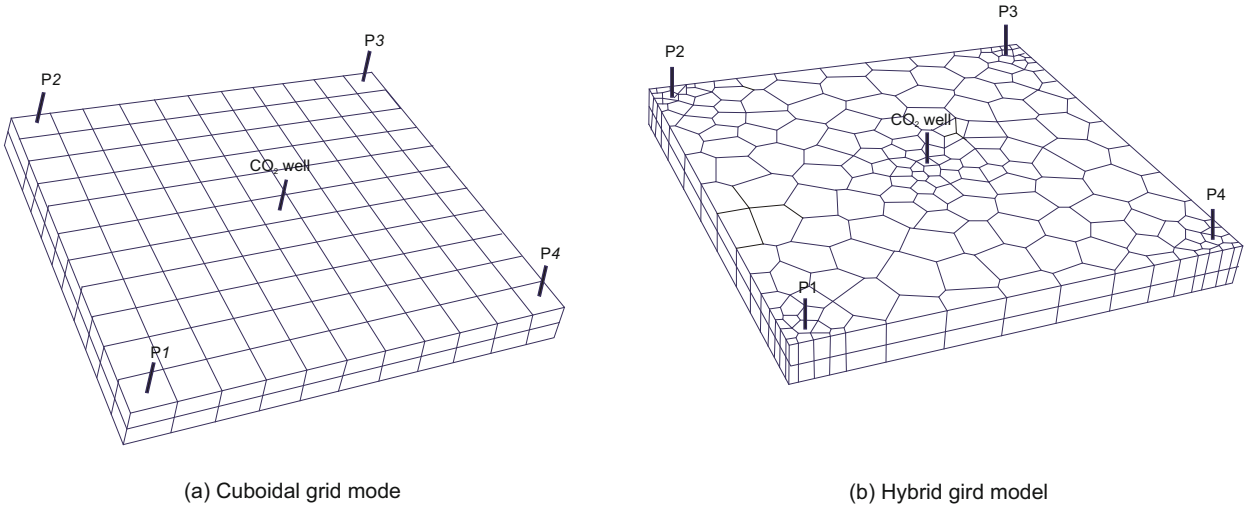

(a) Cuboidal grid mode (b) Hybrid gird model

Fig. 4 Grid types used in simulation sample

Table 3 Main parameters of the two demonstrations

Parameters	Value	Parameters	Value
The length of the geological model *X*, m	220	Initial oil saturation	0.449
The width of the geological mode *Y*, m	220	Initial water saturation	0.551
The thickness of the geological mode *Z*, m	20	Porosity	0.185
Initial reservoir temperature, ºC	99	Permeability for all grids at all direction, 10^{-3} μm^2	90
Initial reservoir pressure, MPa	30.18	CO_2 injection rate of each injection well, kg/s	0.08
Numbers of pseudo-components of oil	5	Wellbore flow pressures for four production wells, MPa	30.01

Fig. 5(a) shows that the apparent distribution of CO_2 in the oil phase is affected by the grid direction. The contours of CO_2 mole fractions around the injection well look like squares. The transport velocities of CO_2 in the oil formation reach a maximum in the *X* and *Y* directions, which demonstrates a numerical pseudo-phenomenon for the cuboidal grid model. The contours of CO_2 mole fractions around the injection well look like circles in Fig. 5(b). The characteristic of the contours reflects radial flow behavior. This implies that the simulation results in this hybrid grid model are more accurate than that in the regular cuboidal grid model.

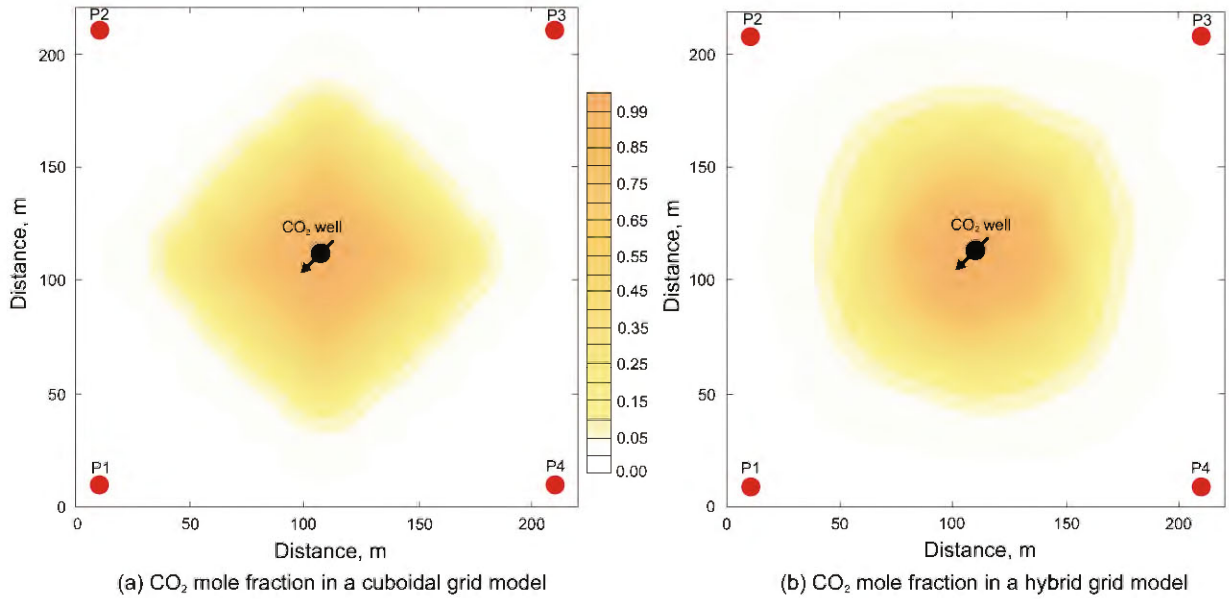

Fig. 5 The distribution of CO_2 in the oil phase after CO_2 injection of 400 days

5 Conclusions

A nonisothermal multi-compositional mathematical model is developed for predicting CO_2 miscible flood in oil reservoirs for EOR. Physical and chemical processes such as heat transfer, multi-component convection-diffusion, adsorption, are fully considered during CO_2 flow and transport in porous media. The governing equations of CO_2 miscible flood are discretized in space using an integral finite-difference method. The Newton-Raphson iterative technique is used to solve the numerical equation system. Slim tube experimental data are used to validate the model and simulator developed in this work. Two simulations of the 3D cuboidal and hybrid grid model demonstrate the optional functions for grid types and their effects on the modeled CO_2 distribution in oil. It is found that the hybrid grid system leads to more accurate prediction of CO_2 distribution than that of the cuboidal grid.

Acknowledgements

Parts of this work were supported by the National Science and Technology Major Projects (2011ZX05009-002, 2011ZX05009–006), the Fundamental Research Funds for the Central Universities, the Project-sponsored by SRF for ROCS, SEM, and the joint research on "Investigation of Mathematical Models and Their Applications for Oil, Water and CO_2 Flow in Reservoirs" between Colorado School of Mines, U.S.A and PetroChina Research Institute of Petroleum Exploration & Development (RIPED), CNPC, China. This support is appreciated.

References

Adewusi V A. Predictive model studies of miscible gas flooding of Nigerian undersaturated crude oil reservoirs. Petroleum Science and Technology. 1998. 16(9-10): 903-929

Barnhart W and Coulthard C. Weyburn CO_2 miscible flood conceptual design and risk assessment. Journal of Canadian Petroleum Technology. 2000. 39(9): 25-33

Dabagh M, Jalali P and Sarkomaa P. The role of micropores structure in conductive and convective heat transfer within porous media. Journal of Porous Media. 2009. 12(4): 301-311

Dahaghi A K, Gholami V and Moghadasi J et al. Formation damage through asphaltene precipitation resulting from CO_2 gas injection in Iranian carbonate reservoirs. SPE Production & Operations. 2008. 23(2): 210-214

Farajzadeh R, Andrianov A and Zitha P L J. Investigation of immiscible and miscible foam for enhancing oil recovery. Industrial & Engineering Chemistry Research. 2009. 49(4): 1910-1919

Ju B, Dai S, Luan Z, et al. A study of wettability and permeability change caused by adsorption of nanometer structured polysilicon on the surface of porous media. Paper SPE 77938 presented at SPE Asia Pacific Oil and Gas Conference and Exhibition, Melbourne, Australia, 2002

Ju B S and Fan T L. Experimental study and mathematical model of nanoparticle transport in porous media. Powder Technology. 2009. 192 (2): 195-202

Ju B S, Fan T L, Wang X D et al. A new simulation framework for predicting the onset and effects of fines mobilization. Transport in Porous Media. 2007. 68(2): 265-283

Mungan N. Carbon-dioxide flooding as an enhanced oil-recovery process. Journal of Canadian Petroleum Technology. 1992. 31(9): 13-15

Orr F M, Heller J P and Taber J J. Carbon dioxide flooding for enhanced oil recovery: Promise and problems. Journal of the American Oil Chemists' Society. 1982. 59(10): 810A-817A

Özkilic Ö İ and Gumrah F. Simulating CO_2 sequestration in a depleted gas reservoir. Energy Sources, Part A: Recovery Utilization and Environmental Effects. 2009. 31(13): 1174-1185

Pruess K. A TOUGH2 fluid property module for mixtures of water, NaCl, and CO_2. Technical Report. Lawrence Berkeley National Laboratory, 2005

Rackley S A. Carbon Capture and Storage. USA Elsevier Inc: Burlington, 2010. 5-6

Scheidegger A E. General theory of dispersion in porous media. Journal of Geophys Research. 1961. 66(10): 3273-3278

Scott D M, Das D K, Subbaihaannadurai V, et al. A computational

scheme for fluid flow and heat transfer analysis in porous media for recovery of oil and gas. Petroleum Science and Technology. 2005. 23 (7-8): 843-862

Song D W. Main influencing factors of the numerical simulation result with CO_2 miscible displacement. Petroleum Geology and Recovery Efficiency. 2008. 15(4): 72-74 (in Chinese)

Su Y L, Wu X D, Hou Y H, et al. Mechanism of CO_2 miscible displacement in low permeability reservoirs and influencing factor. Journal of China University of Petroleum. 2011. 35(3): 99-102 (in Chinese)

Wang J, Cai B, Cao D, et al. Scenario study of regional allocation of CO_2 emissions allowance in China. Acta Scientiae Circumstantiae. 2011. 31(4): 680-685 (in Chinese)

Wells A W, Diehl J R, Bromhal G, et al. The use of tracers to assess leakage from the sequestration of CO_2 in a depleted oil reservoir, New Mexico, USA. Applied Geochemistry. 2007. 22(5): 996-1016

Wu Y S and Pruess K. Numerical simulation of non-isothermal multiphase tracer transport in heterogeneous fractured porous media. Advance in Water Resources. 2000. 23(7): 699-723

Yang F, Bai B J, Tang D Z, et al. Characteristics of CO_2 sequestration in saline aquifer. Petroleum Science. 2010. 7(1): 83-92

Zhao Y C, Song Y C, Liu Y, et al. Visualization of CO_2 and oil immiscible and miscible flow processes in porous media using NMR micro-imaging. Petroleum Science. 2011. 8(2): 183-193

(Edited by Sun Yanhua)